

Grating Based Differential Phase Contrast X-Ray Imaging

Joseph Zambelli, Ph.D., Nicholas Bevins, M.S., Ke Li, M.S., Zhihua Qi, M.S., Guang-Hong Chen, Ph.D.

August 3, 2011



DEPARTMENT OF
Medical Physics
UNIVERSITY OF WISCONSIN SCHOOL OF MEDICINE AND PUBLIC HEALTH

Outline

- Background
 - Introduction to phase contrast imaging
 - Talbot-Lau interferometry & phase stepping
- System design
 - X-ray grating fabrication
 - System overview
- Results
 - Phantom results
 - Electron density and atomic number imaging
 - Dark field imaging
 - Tissue sample results



2

Phase Contrast Imaging

- Physical Foundation
 - Electron density can be measured by observing the phase shift of x-rays as they pass through an object

$$\varphi = \frac{2\pi}{\lambda} \int_l \delta(l) dl = \lambda r_e \int_l \rho_e(l) dl$$

- Alternatively, if the refraction angle of the x-ray beam, Θ , is measured, it can be related to the phase shift.

$$\Theta(x, y) = \frac{\lambda}{2\pi} \frac{\partial}{\partial x} \varphi(x, y) = \frac{\partial}{\partial x} \int_l \delta(l) dl$$



3

Similarity to Absorption Imaging

- Note the similarity of the line integral for refraction index decrement to the line integral for standard absorption CT shown below.

$$\Theta(x, y) = \frac{\partial}{\partial x} \int_l \delta(l) dl \quad \ln \frac{I_0}{I} = \int_l \mu(l) dl$$

- This allows us to reconstruct an image of δ , and therefore electron density, using the same approach we use for absorption images.
- The only difference is that a Hilbert filter is used in the reconstruction of δ images instead of a ramp filter.

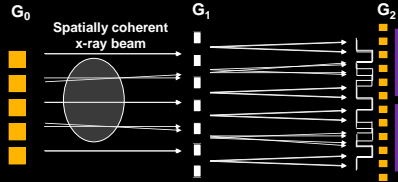
F. Pfeiffer, C. Kottler, O. Bunk, and C. David, "Hard x-ray phase tomography with low-brilliance sources," *Phys. Rev. Lett.* 98(108105), p. 108105, 2007.

Z. Qi and G. H. Chen, "Direct fan-beam reconstruction algorithm via filtered backprojection for differential phase-contrast computed tomography," *X-ray Opt. and Instr.* 53, pp. 1015-25, 2008.



4

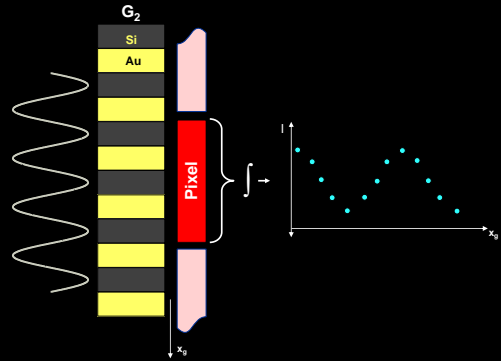
Talbot-Lau Interferometer



F. Pfeiffer, et al. Phase retrieval and differential phase-contrast imaging with low-brilliance x-ray sources
Nature Physics 2, pp. 258–261, Apr 2006

5

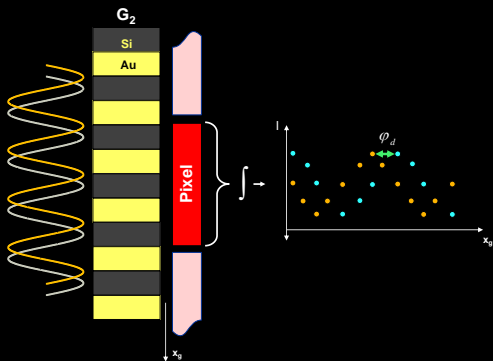
Grating Interferometer



T. Weitkamp, et al. "X-ray phase imaging with a grating interferometer," Opt. Exp. 12(16), pp. 6296–304, 2005.

6

Grating Interferometer



7

Three contrast mechanisms from the same data acquisition

$$I(m, n; x_s) = I_0(m, n) + I_1(m, n) \cos \left[\frac{2\pi}{p_2} x_s + \varphi_d(m, n) \right]$$

- Absorption contrast: The DC term of the measured signal, I_0
- Refraction contrast: Phase offset of the measured signal, φ_d
- Dark field contrast: Amplitude of the measured signal, I_1

8

Phase Shift Measurement



- The phase offset is measured when the object is present and when it is not. The difference between the two gives a measurement which is related to the refraction angle through the object.

$$\varphi_d = \varphi_d^{\text{object}} - \varphi_d^{\text{background}}$$

$$\Theta = \frac{p_2}{2\pi d} \cdot \varphi_d$$

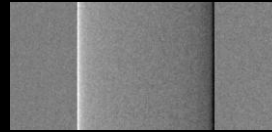
$$\Theta = 4.28 \times 10^{-6} \cdot \varphi_d$$

9

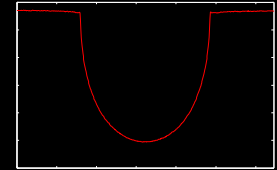
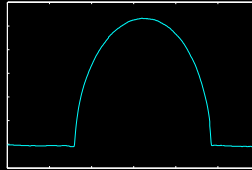
X-ray Grating Interferometry



Differential phase



Absorption



Ke Li, "regularized phase retrieval from DPC projection images" Room 211, 5:40PM

10

Effective Z - μ/δ Ratio



$$\mu \approx \rho_e \left[k_1 \frac{Z^4}{E^3} + k_2 f_{KN}(E) \right] \quad \delta = \frac{\rho_e r_0 \hbar^2 c^2}{2\pi E^2}$$

$$\frac{\mu}{\delta} \approx \frac{2\pi E^2}{r_0 \hbar^2 c^2} \left[k_1 \frac{Z^4}{E^3} + k_2 f_{KN}(E) \right]$$

$$\frac{\mu}{\delta} \approx p \cdot Z^n + q$$

- The ratio reflects information about the effective atomic number of a material. The coefficients of the ratio can be determined by scanning a set of known materials. Decomposition of μ into ρ_e and Z_{eff} may improve material differentiation.

Qi, Z., Zambelli, J., Bevins, N. & Chen, G.-H. Quantitative imaging of electron density and effective atomic number using phase contrast CT. Phys. Med. Biol., 2010, Vol. 55, pp. 2659-2677

11

X-ray Grating Fabrication



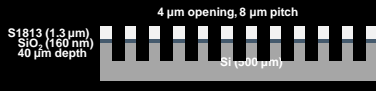
- The addition of gratings is the most important difference from conventional absorption-based imaging systems
- 1D gratings are fabricated in silicon wafers
 - Acceptable x-ray attenuation
 - High quality wafers are readily available at reasonable cost
 - Many well-characterized processes have been developed for silicon
- Basic approach is to transfer a user-defined pattern to the silicon surface and either etch into the wafer or add material to the surface

12

G₁ Fabrication

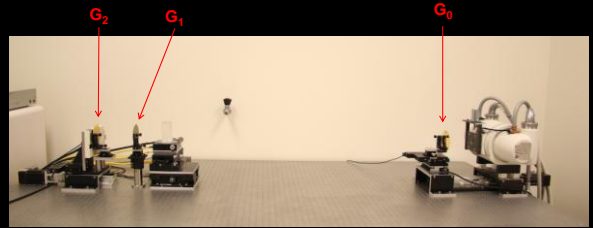


- Outsize $\times 110$- Si wafer at 1050°C
- Wafer bake at 115°C
- Spin coat S1813 photoresist
- Soft bake at 115°C
- Expose for 6 seconds
- Develop in MF-321 for 45 seconds
- Post-development bake at 115°C
- Etch oxide layer in BOE
- Strip S1813 photoresist
- Etch in KOH at 80°C to 40 μm
- Strip oxide layer in BOE



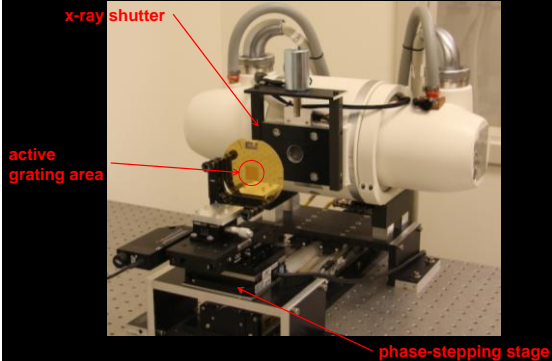
13

X-ray Grating Interferometer – Experimental System



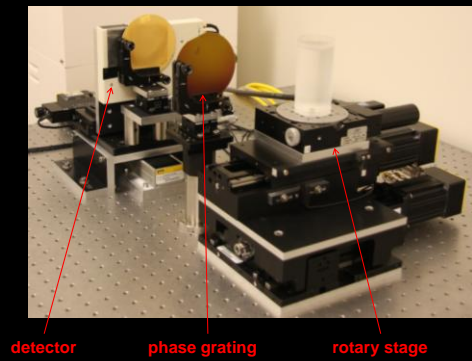
14

X-ray Grating Interferometer – Experimental System



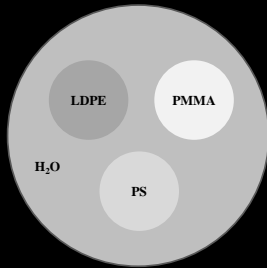
15

X-ray Grating Interferometer – Experimental System



16

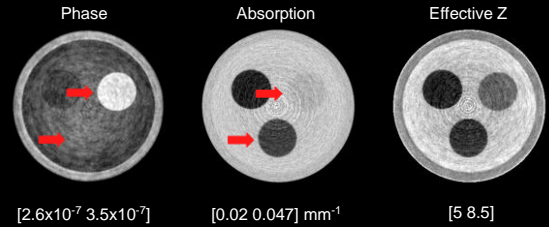
Phantom Results



Phantom is constructed from a 25.5 mm PMMA tube containing 6.2 mm inserts with the remaining volume filled with water.

17

Phantom Results

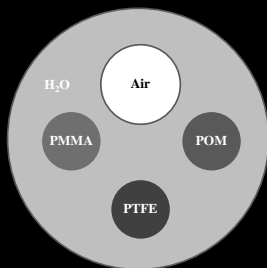


Qi, Z., Zambelli, J., Bevins, N., & Chen, G.-H. Quantitative imaging of electron density and effective atomic number using phase contrast CT. *Phys. Med. Biol.*, 2010, Vol. 55, pp. 2669-2677

Zambelli, J., Bevins, N., Qi, Z., & Chen, G.-H. Measurement of contrast-to-noise ratio for differential phase contrast computed tomography. *Med. Phys.*, 2010, Vol. 37, pp. 2473-2478

18

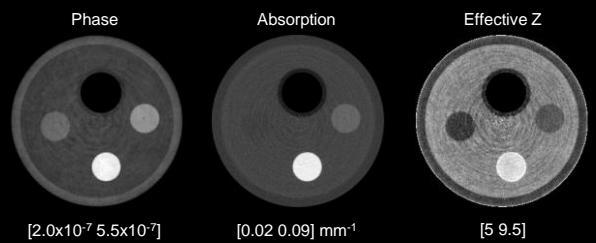
Phantom Results



Phantom is constructed from a 28.5 mm PMMA tube containing 4.8 mm inserts with the remaining volume filled with water.

19

Phantom Results

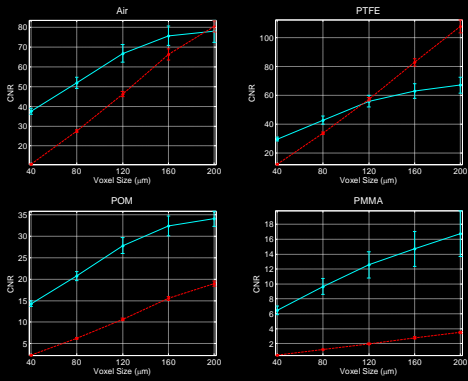


Qi, Z., Zambelli, J., Bevins, N., & Chen, G.-H. Quantitative imaging of electron density and effective atomic number using phase contrast CT. *Phys. Med. Biol.*, 2010, Vol. 55, pp. 2669-2677

Zambelli, J., Bevins, N., Qi, Z., & Chen, G.-H. Measurement of contrast-to-noise ratio for differential phase contrast computed tomography. *Med. Phys.*, 2010, Vol. 37, pp. 2473-2478

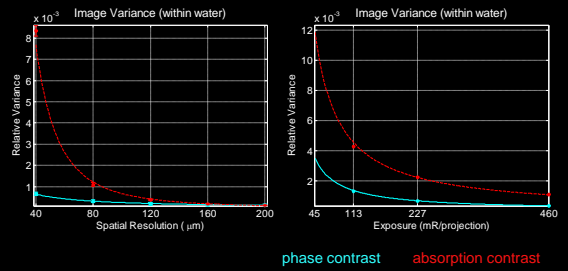
20

Phantom Results – CNR



21

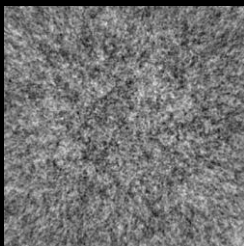
Phantom Results – Noise



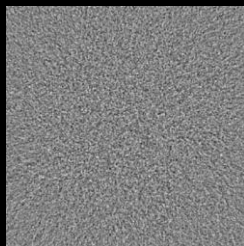
Relative variance is defined as the square of the ratio of image noise to mean signal value. This dimensionless quantity allows comparison between different contrast mechanisms.

22

Noise Comparison



Phase Contrast

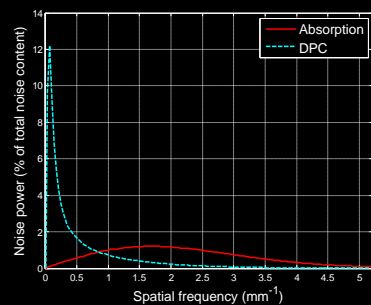


Absorption Contrast

Zambelli, et al., Proc. SPIE, Vol. 7961, 79613N (2011)

23

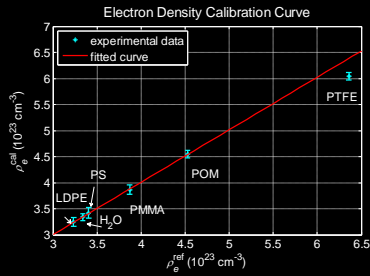
Noise Power Comparison



Zambelli, et al., Proc. SPIE, Vol. 7961, 79613N (2011)

24

Electron Density Calibration



$$\rho_e^{\text{cal}} = a \times \rho_e^{\text{ref}} + b$$

$$a = 1.0055$$

$$b = -0.0123$$

$$R^2 = 0.9996$$

Potential error sources:

- Inaccurate knowledge of the mass density of the materials
- Beam hardening effects

Qi, Z., Zambelli, J., Bevins, N. & Chen, G.-H. Quantitative imaging of electron density and effective atomic number using phase contrast CT. *Phys. Med. Biol.*, 2010, Vol. 55, pp. 2659-2677

25

Effective Z Measurement



	LDPE	PS	PMMA	POM	Water	PTFE
Z_{eff}	5.44	5.70	6.47	6.95	7.42	8.43
μ/δ (10^6 cm^{-1})	0.891	0.923	1.07	1.15	1.26	1.62

- Z_{eff} is calculated using¹

$$Z_{\text{eff}} = 2.94 \sqrt{\sum_i f_i \times (Z_i)^{2.94}}$$

- μ/δ and Z_{eff} are assumed to follow

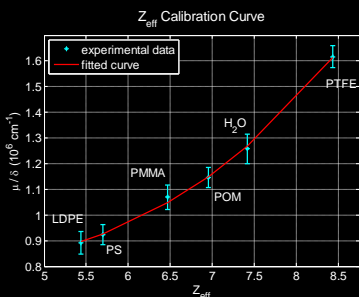
$$\frac{\mu}{\delta} = p \times Z^n + q$$

- A non-linear least squares fit using a quasi-Newton method was applied to determine the parameters.

1. F. W. Spiers, "Effective atomic number and energy absorption in tissues," *British Journal of Radiology* 19, pp. 52-63, 1946.

26

Effective Z Calibration



$$\frac{\mu}{\delta} = p \times Z^n + q$$

$$n = 3.906$$

$$p = 211.9 \text{ cm}^{-1}$$

$$q = 7.375 \times 10^5 \text{ cm}^{-1}$$

$$R^2 = 0.998$$

Qi, Z., Zambelli, J., Bevins, N. & Chen, G.-H. Quantitative imaging of electron density and effective atomic number using phase contrast CT. *Phys. Med. Biol.*, 2010, Vol. 55, pp. 2659-2677

27

Modulation Amplitude



- One term of the equation describing the measured intensity has not yet been used.

$$I(m, n; x_g) = I_0(m, n) + I_1(m, n) \cos \left[\frac{2\pi}{p_2} x_g + \varphi_d(m, n) \right]$$

- This term reflects the amplitude of the intensity change as phase stepping is performed.
- What information can this term provide about the image object?

28

Dark Field Imaging



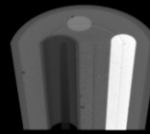
- A dark field image can be extracted using the normalized oscillation amplitude

$$V^{\text{bkgd}}(m, n) \equiv \frac{(I_{\text{max}} - I_{\text{min}})}{(I_{\text{max}} + I_{\text{min}})} = \frac{I_1(m, n)}{I_0(m, n)}$$

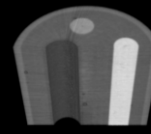
$$V_{\text{SAS}} = \frac{V^{\text{obj}}(m, n)}{V^{\text{bkgd}}(m, n)} = \frac{I_0^{\text{bkgd}}}{I_0^{\text{obj}}} \frac{I_1^{\text{obj}}}{I_1^{\text{bkgd}}}$$

$$\ln(V_{\text{SAS}}) = -\frac{r^2}{4} \int dz \frac{\sigma_{\text{SAS}} \rho_{\text{SAS}}}{R^2(z)}$$

Phantom Results



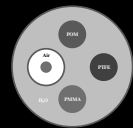
Attenuation



Phase Contrast



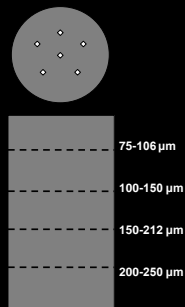
Dark Field



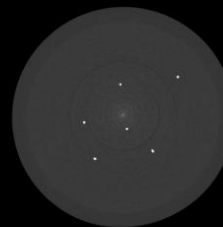
Calcification Phantom



- PMMA cylinder with inner diameter of 22.2 mm and wall thickness of 1.65 mm.
- Calcium hydroxylapatite grains were added in 4 layers.
- Each layer contains a range of sizes, from 200-250 μm , down to 75-106 μm .
- The background material for the phantom is a beef hide gelatin (15 g/100 mL of water).



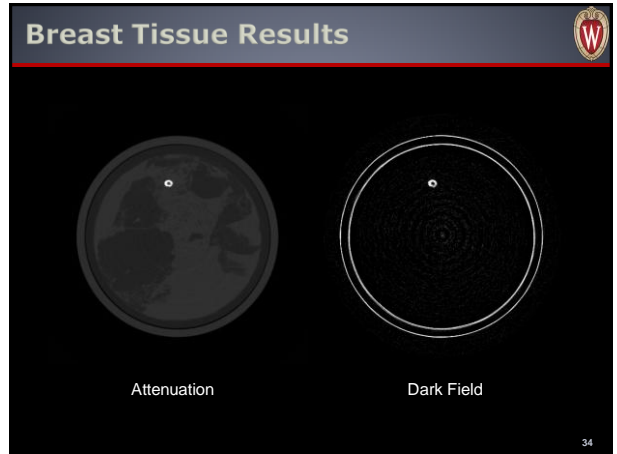
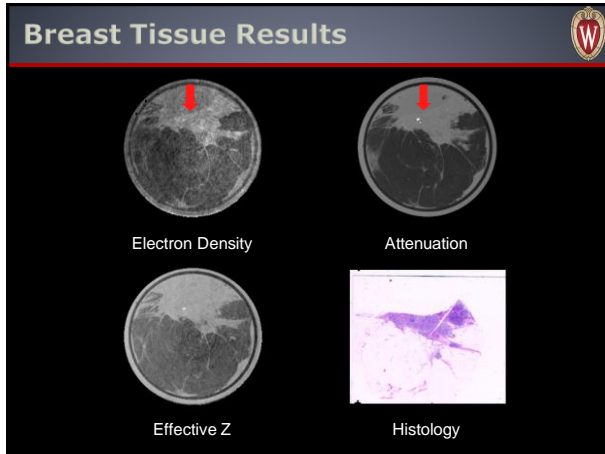
Calcification Phantom



Attenuation



Dark Field



Potential Advantages

- DPC x-ray imaging provides a way to exploit the wave nature of x-rays, allowing simultaneous reconstruction of images of multiple physical quantities.
- The method provides quantitative measurement of electron density, effective atomic number, and attenuation coefficient.
- The relationship between noise and spatial resolution is far less severe for phase contrast imaging than for absorption imaging.
- Phase contrast imaging has potential to achieve low contrast detectability of tissues not possible with conventional absorption imaging.

35

Potential Challenges

- Increased scan time due to phase stepping
 - Use fewer phase steps
 - Alternative schemes require no phase steps
 - Compressed sensing techniques may reduce view sampling requirements
- Grating fabrication is technically challenging for higher operating energies and compact systems
 - New microfabrication techniques and scanning geometries can help address this
- Tube loading from absorption gratings
 - Use of large focal spots allows operation at high peak power

36



Thanks for your attention!



UWCT